FISEVIER

Contents lists available at ScienceDirect

# Journal of Alloys and Compounds

journal homepage: www.elsevier.com/locate/jalcom



# Magnetic properties of $SmCo_{5-x}Fe_x$ (x = 0-4) melt-spun ribbon



Tetsuji Saito <sup>a,\*</sup>, Daisuke Nishio-Hamane <sup>b</sup>

- <sup>a</sup> Department of Mechanical Science and Engineering, Chiba Institute of Technology, 2-17-1 Tsudanuma, Narashino, Chiba 275-0016, Japan
- <sup>b</sup> Institute for Solid State Physics, The University of Tokyo, 5-1-5 Kashiwanoha, Kashiwa, Chiba 277-8581, Japan

### ARTICLE INFO

Article history:
Received 26 August 2013
Received in revised form 25 September 2013
Accepted 26 September 2013
Available online 9 October 2013

Keywords: Sm-Co magnets Melt-spinning Nanocomposite TEM

#### ABSTRACT

 $SmCo_{5-x}Fe_x$  (x=0-4) alloys were produced by melt-spinning and subsequent annealing. It was found that the small substitution of Fe for Co in the  $SmCo_5$  alloy results in the formation of the  $Sm(Co,Fe)_5$  phase, but that the large substitution of Fe for Co results in the formation of other phases such as the  $Sm(Co,Fe)_7$  and  $Sm_2(Co,Fe)_7$  phases. The remanence of the annealed  $SmCo_{5-x}Fe_x$  melt-spun ribbons increased from x=0 to x=3 then decreased with increasing Fe content, while their coercivity decreased as the Fe content increased. Transmission electron microscope (TEM) studies revealed that the annealed  $SmCo_4Fe$  melt-spun ribbon consisted of relatively coarse  $Sm(Co,Fe)_5$  grains, whereas the annealed  $SmCo_2Fe_3$  melt-spun ribbon consisted of a mixture of extremely fine grains of the  $Sm(Co,Fe)_7$  and Fe phases. The annealed  $SmCo_4Fe$  alloy with the  $Sm(Co,Fe)_5$  phase showed a high coercivity of 10.2 kOe with a remanence of 60 emu/g, while the annealed  $SmCo_2Fe_3$  alloy formed a nanocomposite magnet with a high remanence of 100 emu/g and a coercivity of 2.9 kOe.

© 2013 Elsevier B.V. All rights reserved.

## 1. Introduction

Since it was found that Nd-Fe-B permanent magnets exhibit excellent hard magnetic properties, research and development of new permanent magnetic materials has largely concentrated on rare-earth-containing alloys [1,2]. As a result of intensive research on such alloys, various new rare-earth intermetallic compounds have been produced such as the RFe<sub>12</sub>, R<sub>3</sub>Fe<sub>29</sub>, and R<sub>5</sub>Fe<sub>17</sub> phases [3–5]. Because the binary RFe<sub>12</sub> and  $R_3$ Fe<sub>29</sub> phases are metastable, the formation of these phases is rather difficult. It has been found that the small substitution of Fe for M (M: transition metal) in the RFe<sub>12</sub> and R<sub>3</sub>Fe<sub>29</sub> phases results in the formation of the R(Fe,M)<sub>12</sub> and  $R_3(Fe,M)_{29}$  phases [6–11]. However, the magnetic properties of these compounds are inferior to those of Nd-Fe-B magnets. In the case of the R<sub>5</sub>Fe<sub>17</sub> phase, the binary Sm<sub>5</sub>Fe<sub>17</sub> phase has been produced by melt-spinning. The coercivity of the Sm<sub>5</sub>Fe<sub>17</sub> phase is much larger than that of Nd-Fe-B magnets, but its remanence is much lower [12,13]. The outlook for the discovery of new magnetic phases with magnetic properties comparable to those of Nd-Fe-B magnets is therefore not promising.

Another approach is to improve the magnetic properties of nanocomposite magnets, one of the new types of permanent magnets [14]. Nanocomposite magnets are composed of a mixture of nanosize soft magnetic and hard magnetic phases. It is known that the existence of the soft magnetic phase in a permanent magnet weakens the remanence and maximum energy product. Due to

E-mail address: tetsuji.saito@it-chiba.ac.jp (T. Saito).

exchange coupling of the nanosize soft magnetic and hard magnetic phases, nanocomposite magnets exhibit a higher remanence than conventional magnets. Anisotropic nanocomposite magnets are expected to show giant maximum energy products as high as  $1 \text{ MJ/m}^3$  when the soft magnetic and hard magnetic phases are arranged in the optimal manner [15]. Since the coercivity of nanocomposite magnets is highly dependent on the coercivity of the hard magnetic phase, a hard magnetic phase with high coercivity such as the SmCo $_5$  phase is desirable as the hard magnetic phase in these magnets. Thus, the production of SmCo $_5$ -based nanocomposite magnets by mechanical alloying has been studied [16–19].

Nanocomposite magnets can be produced not only by mechanically alloying but also by melt-spun spinning [20–24]. In the present study,  $SmCo_{5-x}Fe_x$  (x = 0–4) alloys were produced by the melt-spinning technique. The purpose of this study was to seek the possibility of producing  $SmCo_5$ -based nanocomposite magnets by melt-spinning and subsequent annealing. The structures and magnetic properties of the resultant Sm-Co-Fe melt-spun ribbons are discussed here.

## 2. Experimental

 $SmCo_{5-x}Fe_x$  (x = 0–4) alloy ingots were prepared by induction melting of Sm (99.9 wt%), iron (99.9 wt%), and cobalt (99.9 wt%) under an argon atmosphere. An alloy ingot of 20 g was induction melted under an argon atmosphere in a quartz crucible having an orifice of 0.6 mm in diameter at the bottom. The molten metal was ejected through the orifice with argon onto a chromium-plated copper wheel rotating at a surface velocity of 50 ms $^{-1}$ . The resultant melt-spun ribbons were obtained as fragmented pieces (thickness:  $10~\mu m$ ; width: 1~mm). In spite of the high oxidation tendency of Sm-containing alloys, the melt-spun ribbons had a smooth

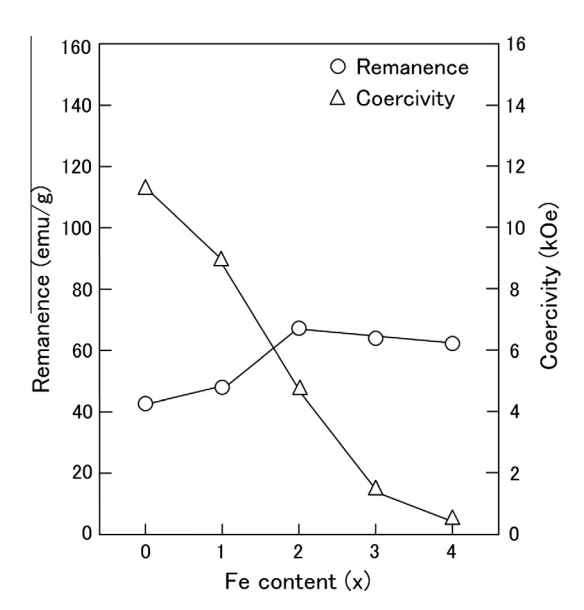
<sup>\*</sup> Corresponding author.

metallic surface. The melt-spun ribbons were wrapped with tantalum foil and annealed under an argon atmosphere for 5 min at temperatures between 673 K and 1073 K. The phases in the specimens were examined by X-ray diffraction (XRD) using Cu K $\alpha$  radiation. The microstructures of the specimens were examined using a transmission electron microscope (TEM) after ion-beam thinning. The thermomagnetic curves of the specimens were examined by heating them at a rate of 0.16 K/s in a vacuum using a vibrating sample magnetometer (VSM) with an applied field of 500 Oe. The VSM was calibrated with a pure nickel sphere. The slope of the thermomagnetic curve near the Curie temperature was determined by curve fitting and the Curie temperature was determined by extraplolation. The magnetic properties of the specimens were measured at room temperature by the VSM with a maximum applied field of 25 kOe.

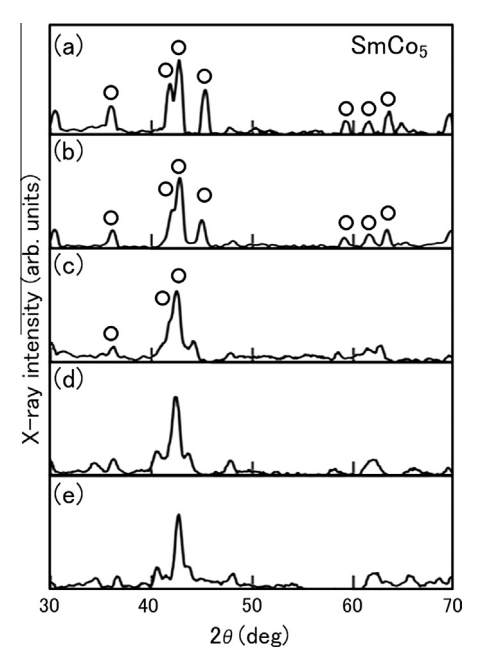
#### 3. Results and discussion

Fig. 1 shows the dependence of the remanence and coercivity of the  $SmCo_{5-x}Fe_x$  (x=0-4) melt-spun ribbons on the Fe content. The  $SmCo_5$  alloy melt-spun ribbon exhibited a high coercivity of 11.2 kOe and a remanence of 42 emu/g. As can be seen in the figure, the remanence of the  $SmCo_{5-x}Fe_x$  (x=0-4) melt-spun ribbons increases up to x=2 then gradually decreases as the Fe content increases. However, the coercivity monotonically decreases with increasing Fe content. It was found that the substitution of Fe for Co in the  $SmCo_5$  alloy increased the remanence but resulted in a significant decrease in coercivity.

The structures of the Sm-Fe-Co melt-spun ribbons were examined by XRD and thermomagnetic studies to evaluate the differences in remanence and coercivity. The results are shown in Figs. 2 and 3, respectively. The SmCo<sub>5</sub> alloy shows diffraction peaks assigned to the SmCo<sub>5</sub> phase and its thermomagnetic curve shows one magnetic transition at around 1010 K, which corresponds to the Curie temperature of the SmCo<sub>5</sub> phase [25]. This confirms that the SmCo<sub>5</sub> alloy consists of the SmCo<sub>5</sub> phase. The XRD patterns of the SmCo<sub>4</sub>Fe and SmCo<sub>3</sub>Fe<sub>2</sub> alloys are somewhat similar in appearance to that of the SmCo<sub>5</sub> alloy, and their thermomagnetic curves are also similar, confirming that these alloys consist of a SmCo<sub>5</sub>type phase such as the Sm(Co,Fe)<sub>5</sub> phase. On the other hand, the XRD patterns of the SmCo<sub>2</sub>Fe<sub>3</sub> and SmCoFe<sub>4</sub> alloys differ from that of the SmCo<sub>5</sub> alloy. This suggests that the large substitution of Fe for Co in the SmCo<sub>5</sub> alloy resulted in the formation of a different phase, not the SmCo<sub>5</sub>-type phase. The XRD pattern of the SmCo<sub>2</sub>Fe<sub>3</sub> alloy was somewhat indexed to a SmCo<sub>7</sub>-type phase; in this case, the Sm(Co,Fe)<sub>7</sub> phase. The Curie temperature of the Sm(Co,Fe)<sub>7</sub>



**Fig. 1.** Dependence of the remanence and coercivity of the  $SmCo_{5-x}Fe_x$  (x = 0-4) melt-spun ribbons on the Fe content.



**Fig. 2.** XRD patterns of the Sm-Co-Fe melt-spun ribbons: (a)SmCo<sub>5</sub>, (b) SmCo<sub>4</sub>Fe, (c) SmCo<sub>2</sub>Fe<sub>3</sub>, (d) SmCo<sub>2</sub>Fe<sub>3</sub> and (e) SmCoFe<sub>4</sub> alloys.

phase is around 910 K, which is much lower than the reported Curie temperature of the  $SmCo_7$  phase is of around 1050 K [26]. It has been reported that the substitution of Ni for Co in  $SmCo_7$  alloy leads to a significant decrease in the Curie temperature of the  $Sm(Co,Ni)_7$  phase [27]. The observed lower Curie temperature of the  $Sm(Co,Fe)_7$  phase is believed to be due to the substitution of Fe for Co in the  $SmCo_7$  alloy. The XRD pattern of the  $SmCoFe_4$  alloy is similar to that of the  $SmCo_2Fe_3$  alloy, but the thermomagnetic curve is quite different. The magnetic transition at 730 K in the thermomagnetic curve of the  $SmCoFe_4$  alloy corresponds to the

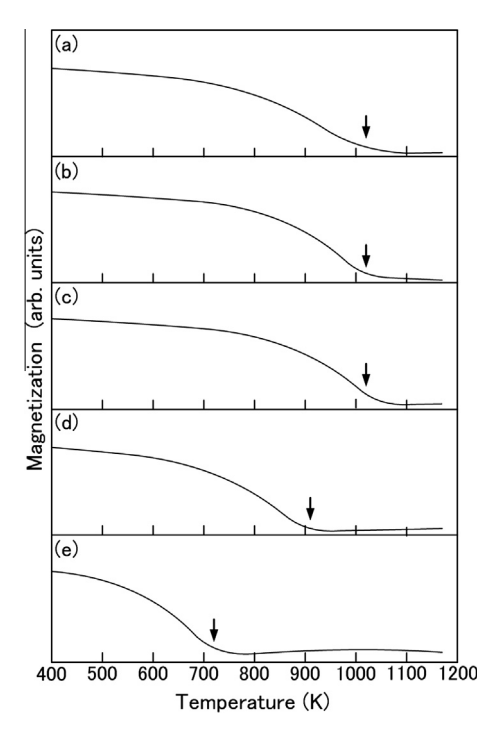


**Fig. 3.** Thermomagnetic curves of the Sm-Co-Fe melt-spun ribbons: (a)SmCo<sub>5</sub>, (b) SmCo<sub>4</sub>Fe, (c) SmCo<sub>3</sub>Fe<sub>2</sub>, (d) SmCo<sub>2</sub>Fe<sub>3</sub> and (e) SmCoFe<sub>4</sub> alloys.

# Download English Version:

# https://daneshyari.com/en/article/1612998

Download Persian Version:

https://daneshyari.com/article/1612998

<u>Daneshyari.com</u>